THE JOURNAL OF PHYSICAL CHEMISTRY B

ARTICLE

pubs.acs.org/JPCB

On the Distribution Functions of Depletion Interactions

Davide Bertolini

Istituto per i Processi Chimico-Fisici, Consiglio Nazionale delle Ricerche, Via G. Moruzzi 1, I-56124 Pisa, Italy

Giorgio Cinacchi[†]

School of Chemistry, University of Bristol, Cantock's Close, Bristol BS8 1TS, England

Alessandro Tani*

Dipartimento di Chimica, Università di Pisa, Via Risorgimento 35, I-56126 Pisa, Italy

ABSTRACT: Molecular dynamics computer simulations were performed on model colloidal binary mixtures of two large and many small soft repulsive spheres. Depletion forces arise between the two large spheres, as a function of their distance, because of the nonadditivity of the volume they exclude to the small spheres. The probability distribution functions of both longitudinal and transverse component of the total force exerted by the small particles were calculated and generally turned out non-Gaussian. The distributions of the collective forces were analyzed in terms of the distribution of the force that a single small sphere exerts on a large sphere and of the number of the surrounding small spheres. The reconstructed function matches well the corresponding exact distribution. Residual correlation among small particles, combined with a relatively small number of neighbors, slows the approach to the Gaussian limit. In our fully repulsive model, the direct force between a large and a small sphere is a monotonic function of their distance. On these bases, we propose and successfully test an approach that relates the probability distribution function of the depletion forces to the large-sphere−small-sphere radial distribution function. This approach can be extended to experimental data of radial distribution function, thus allowing for an estimate of depletion force fluctuations in real colloidal mixtures.

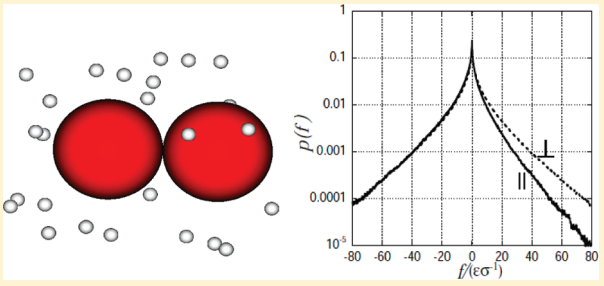

1. INTRODUCTION

Depletion interactions[1,2] arise between two or more large objects when they are immersed in a sample of small depletant particles. Even when the interactions between the constituents of the system are purely repulsive, attractive effective interactions[3,4] between the large objects originate because of the nonadditivity of the excluded volumes involved. In fact, the volume that the large objects jointly excludes to the small particles when the large objects are sufficiently close to each other is smaller than the sum of the volumes excluded by each single large object to the small particles. The latter have therefore more free volume available as the large objects approach.

These effective interactions have proven a useful concept to rationalize the phase behavior of colloid−polymer[1,2] and colloid−colloid mixtures.[5,6] In these cases, large colloidal particles play the role of the above-mentioned large objects, while the polymers or small colloidal particles are the depletants. These effective interactions have been calculated by theoretical (e.g., integral equation[7] and density functional[8] theories) and computer simulation techniques (e.g., refs 9−11) and measured in several experiments (e.g., refs 12−16).

What are called depletion interactions actually are mean interactions. To characterize them further, a knowledge of their probability distribution function (pdf) is desirable. (Similar comments were made in ref 17 where the pdf of Casimir-like forces, induced by thermal fluctuations, was calculated.) In the vast majority of the above-mentioned studies, attention was given to the calculation or measuring of the depletion forces and the associated depletion potential energy functions.

Despite the rich literature accumulated on the depletion interactions, that is, the mean or first moment of the corresponding pdf, the subsequent higher moments have been rarely considered. It would appear that only in ref 18 have the fluctuations of the depletion interactions been given attention by both a scaling theory and Brownian Dynamics simulations. It would also appear that no attention has been given to the entire form of the pdf's of the depletion forces.

These pdf's are expected to play a role in the comprehension of the dynamics in the above-mentioned complex mixtures, and a knowledge of their form together with the devise of a procedure to determine them experimentally are germinal steps in that direction.

Received: January 18, 2011
Revised: April 12, 2011
Published: May 03, 2011

dx.doi.org/10.1021/jp2005259 | *J. Phys. Chem. B* 2011, 115, 6608–6615

In fact, depletion forces are closely related to the fluctuating force, which is responsible for the drag experienced by a colloidal particle moving in a medium. The time correlation function of this random force defines the drag in the Langevin description of the dynamics of these systems. Although in the standard treatment this stochastic process is assumed Gaussian, with a δ function time dependence, it appears worth assessing the scope and accuracy of this hypothesis.

Therefore, a careful analysis of fluctuations may help in building physically sound approximations in the context of coarse-grained descriptions of complex systems, an approach actively pursued to extend the time and size scale of phenomena studied by computer simulation.[19,20]

From a more fundamental point of view, the interest in the fluctuations of depletion forces also stems from their relationship with the response to external perturbations and hence to nonequilibrium processes.[21]

In the present work, model colloid−colloid mixtures are considered in which two large and soft repulsive spheres are immersed in a bath of small soft repulsive spheres. This choice excludes many-body depletion interactions from our study, so that our results and conclusions should be applicable, strictly speaking, to dilute colloidal suspensions.

The two large spheres together with their nearest neighbor small spheres can be seen as an open small system, with the other small spheres acting as a reservoir. Systems of this size are certainly far from the thermodynamic limit, and for them fluctuations are important.[22,23]

The pdf's of the depletion interactions parallel and perpendicular to the axis joining the two large particles have been calculated via Molecular Dynamics (MD) computer simulations. Details of the model and of the MD simulations performed are given in section 2. Results as a function of the distance between the large spheres are presented in section 3.1, where also the effects of the depletant density, size ratio between large and small particles, and degree of softness of the direct interactions are considered. Because depletion interactions are collective in character, the calculated pdf's have been analyzed and reconstructed in terms of the distribution function of the force between a single small sphere and a large sphere. These results are presented in section 3.2, where the possibility to exploit them to experimentally access the pdf's in real colloidal mixtures is also discussed. Finally, section 4 provides a summary and a few concluding comments.

2. MODEL AND MOLECULAR DYNAMICS COMPUTER SIMULATIONS

The model systems considered are formed by two large spherical particles held at a fixed distance and immersed in a bath of small spherical particles. The interaction, $u_{ij}(r)$, between two small spheres or a large and a small sphere is soft repulsive (eq 1):

$$u_{ij}(r) = \begin{cases} 4\varepsilon\left[\left(\frac{\sigma_{ij}}{r}\right)^{2n} - \left(\frac{\sigma_{ij}}{r}\right)^{n} + \frac{1}{4}\right], r \le 2^{1/n}\sigma_{ij} \\ 0, r > 2^{1/n}\sigma_{ij} \end{cases} \quad (1)$$

In eq 1, i and j refer to a pair of interacting particles, and r is the distance separating their centers. If $i = 1$, the particle is a large sphere; if $i = 2$, the particle is a small sphere. The contact distance parameter σ_{ij} is such that: $\sigma_{12} = (\kappa + 1)/2\sigma$ and $\sigma_{22} = \kappa\sigma$ with σ the unit of length and κ a number <1. The parameter κ coincides with the size ratio σ_{22}/σ_{11}, with $\sigma_{11} = \sigma$ the contact distance parameter in the interaction between two particles of type 1 if they too were interacting via eq 1. The quantity ε is the unit of energy, while the exponent n regulates the softness of the interactions.

The two large spheres were placed in the simulation box together with a number, N, of small spheres. N varied between 500 and 15 000. These collections of particles were then simulated via the MD technique at constant volume, V, and temperature, T.[24] While a single value of mean temperature was considered, $T^* = k_BT/\varepsilon = 0.8$ (k_B is the Boltzmann constant), the maintenance of which was achieved by the weak coupling method,[25] numerous values of the density of small spheres, $\rho^* = \rho\sigma_{22}^3$, distance between the centers of the two large particles, R_{11}, and the values of the exponent n were examined. For each simulation run performed, the distance between the two large spheres was maintained fixed at the preselected value by the SHAKE method,[26] while the equations of motion were integrated with the leapfrog version of the Verlet algorithm. The duration of the time step adopted was always 0.00233 in units $t^* = (m/\varepsilon)^{1/2}\sigma$, with m the mass of a small particle. The simulations were performed with a properly modified version of the free MD program package MOSCITO.[27]

Starting configurations were generated via different procedures: directly taken from previous simulations,[11] or generated from a previous higher density configuration either by removing a number of small spheres to achieve the desired value of density, or by slowly varying the contact distance parameter σ_{22} to achieve the desired value of κ. Typical equilibration runs lasted 50−200 thousand time steps. Each of them was followed by a production run of at least as many time steps. During these production runs, the various quantities of interest were calculated.

The depletion force, $F(t)$, is a mean force, the derivative of the potential of mean force, which measures the (reversible) work required to bring the two large spheres to the selected distance from infinite separation, where the potential is assumed to vanish. Among the methods to calculate potentials of mean force, the so-called blue-moon ensemble method, proposed by Ciccotti et al.,[28] is particularly convenient for our purposes. At each time step, the total force exerted by the small spheres onto each large sphere was separated into the longitudinal and transverse component, with respect to the axis joining the centers of the large spheres. The transverse component, $F_\perp(t)$, vanished because of the cylindrical symmetry of the system, while the longitudinal component, $F_\parallel(t)$, gave rise to the depletion force we are interested in.

The corresponding distribution functions, $D(|F|)$, $D_\parallel(F_\parallel)$, and $D_\perp(F_\perp)$, were calculated by accumulating the value of $|F|$, $F_\parallel$, and $F_\perp$ in histograms of width 0.033−0.166 in units ε/σ. Together with these distributions of the depletion force, the distribution functions of the modulus of the direct force that a single small sphere exerted on a large sphere, $p(|f|)$, along with those of its parallel and perpendicular components, $p_\parallel(f_\parallel)$ and $p_\perp(f_\perp)$, were also calculated.

In the following section, the results are presented and discussed.

3. RESULTS AND DISCUSSION

3.1. Distributions of the Depletion Interactions: Effect of the Large Sphere Distance and Small Sphere Density. The

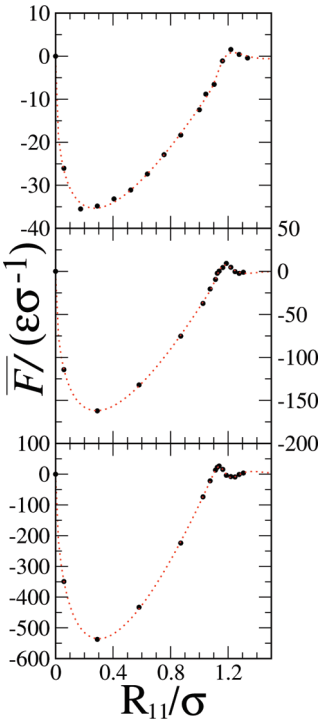

Figure 1. Depletion force, $\overline{F}$, in units of ε/σ, between two large particles (●) as a function of their distance, R_{11}, in units of σ, for three different values of density of small particles: $\rho_{22}^3 = 0.20$ (top panel); $\rho_{22}^3 = 0.45$ (central panel) $\rho_{22}^3 = 0.75$ (bottom panel). Notice the change of the scale of the ordinates in the three panels. The dotted lines are fits to the data; the functional form of the fitting function is described in ref 11.

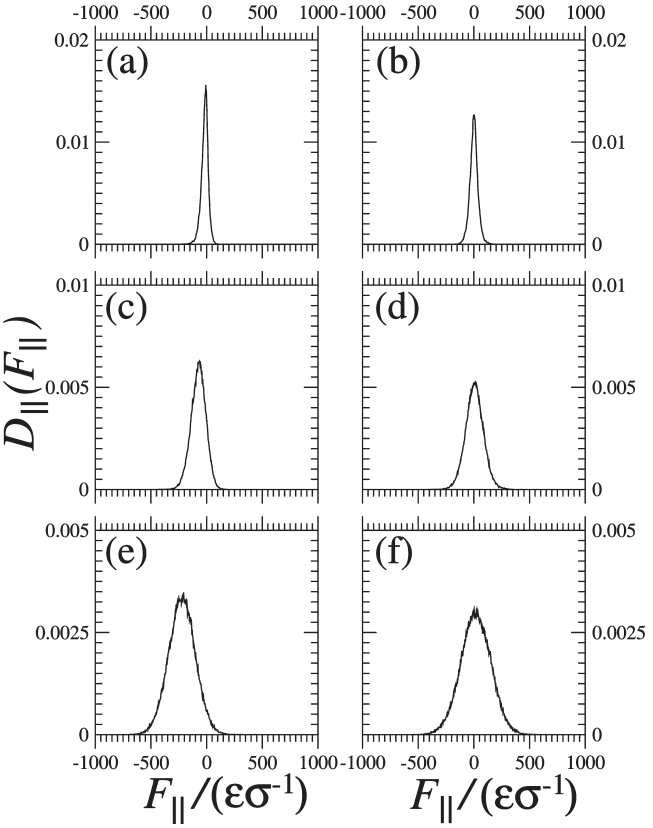

Figure 2. Distribution functions of the longitudinal depletion force, $D_{\|}(F_{\|})$ for various values of density and distance: (a) $\rho^* = 0.20$, $R_{11} = 0.87$; (b) $\rho^* = 0.20$, $R_{11} = 1.16$; (c) $\rho^* = 0.45$, $R_{11} = 0.87$; (d) $\rho^* = 0.45$, $R_{11} = 1.16$; (e) $\rho^* = 0.75$, $R_{11} = 0.87$; (f) $\rho^* = 0.75$, $R_{11} = 1.16$.

changes in the form of the depletion force distributions with the distance between the two large spheres and the density of the small spheres are surveyed. The results presented were obtained using $\kappa = 0.2$ and $n = 6$. MD simulations were conducted at many values of R_{11}. For each of these distances, three values of ρ^* were considered: 0.20, 0.45, 0.75. These values have been selected as they correspond to quite different physical states of the bulk mixture. According to a previous study,[11] at $\rho^* = 0.20$ a completely mixed fluid phase is predicted to be stable for a wide range of density of large spheres. Further increasing ρ^*, an equilibrium is established between a fluid phase almost devoid of large spheres and a crystal phase where the latter are the vast majority component. The values of $\rho^* = 0.45$ and 0.75 correspond to the values of density of depletants at which, respectively, this scenario is going to happen and is definitely realized.

Figure 1 illustrates the dependence of the depletion force, that is, the mean of the parent distribution, $\overline{F}$, on R_{11}, for the three above-mentioned values of ρ^*. For symmetry reasons, $\overline{F}$ coincides with the mean force along the direction joining the centers of the two large spheres, $\overline{F}_{\|}$, while the mean force along a transverse direction, $\overline{F}_{\perp}$, is naturally zero. Curves similar to those displayed in Figure 1 have been already commented on in ref 11. In essence, two distinct regimes characterize them: an attractive, broad minimum at shorter distances, whose depth increases with density, followed by a tail, oscillating around zero and whose amplitude, of magnitude much smaller than the depth of the preceding minimum, fades with distance.

Figures 2 and 3 provide the distribution functions of the depletion force calculated at the following values of R_{11}: 0.87 and 1.16. These values of distances have been selected as representatives of the two above-mentioned regimes. Both the longitudinal, $D_{\|}(F_{\|})$, and the transverse, $D_{\perp}(F_{\perp})$, distributions are given for the three above-mentioned values of density of depletants.

The function $D_{\|}(F_{\|})$ is generally asymmetric and therefore non-Gaussian. The probability density of those values of $F_{\|}$ that are more negative, that is, more attractive, than the mean has a longer tail than the probability density for those values of $F_{\|}$ that are more positive, that is, more repulsive, than the mean. The function $D_{\perp}(F_{\perp})$ is symmetric with respect to $\overline{F}_{\perp}$. Nevertheless, it too is generally non-Gaussian. One way to appreciate this is by fitting the curve to a stretched exponential function of the type: $Ae^{-(|F_{\perp}|/B)^{\beta}}$, with β, A, and B as fitting parameters. The exponent β is generally distinct from 2, particularly for small values of ρ^* and small values of R_{11}. Figure 4 illustrates these considerations. This figure provides, on a logarithmic scale, $D_{\|}(F_{\|})$ and $D_{\perp}(F_{\perp})$ for $\rho^* = 0.20$ and $R_{11} = 1$. One can notice the asymmetry of the longitudinal distribution as well as appreciate the fact that a stretched exponential function with an exponent $\beta = 1.5$ better represents the tails of the transverse distribution than does a Gaussian function.

Expectedly, the Gaussian limit is approached as the density of depletant and the separation between the two large spheres increase. The central limit theorem states that the distribution function of the sum of N indipendent and identically distributed variables turns out to be the Gaussian distribution for $N \rightarrow \infty$, irrespective of the form of the distribution function of these variables, provided the latter pdf has a finite variance. However,

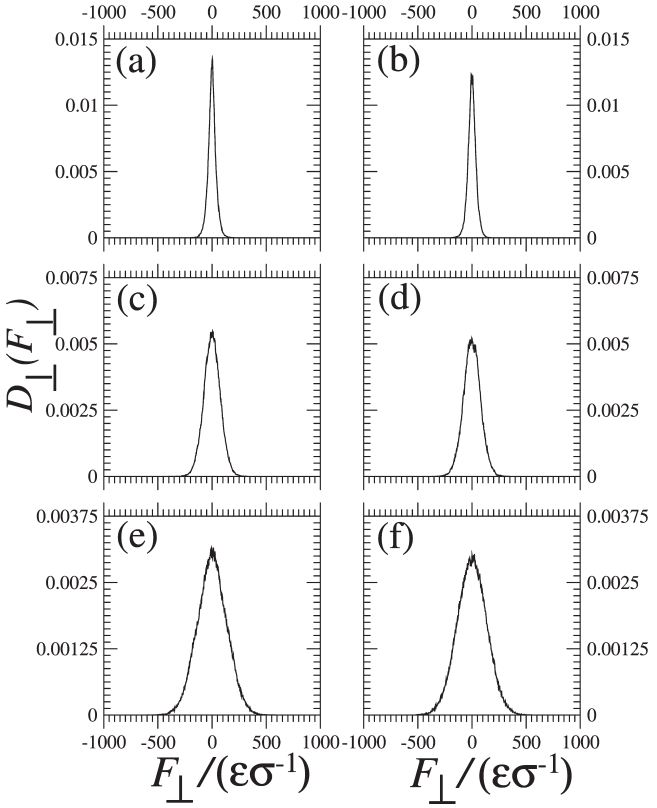

Figure 3. Distribution functions of the transverse depletion force, $D_\perp(F_\perp)$ for various values of density and distance: (a) $\rho^* = 0.20$, $R_{11} = 0.87$; (b) $\rho^* = 0.20$, $R_{11} = 1.16$; (c) $\rho^* = 0.45$, $R_{11} = 0.87$; (d) $\rho^* = 0.45$, $R_{11} = 1.16$; (e) $\rho^* = 0.75$, $R_{11} = 0.87$; (f) $\rho^* = 0.75$, $R_{11} = 1.16$.

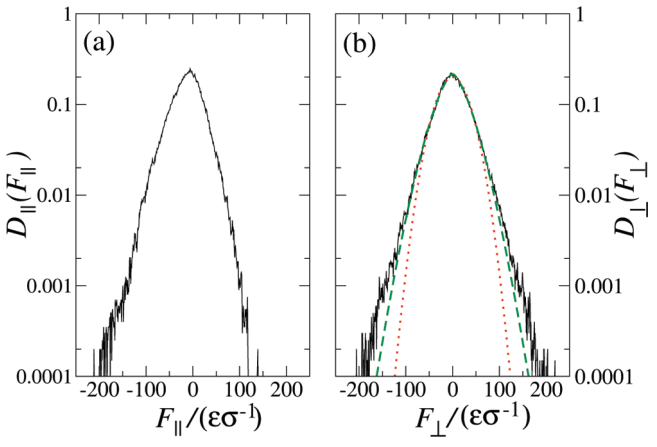

Figure 4. (a) Distribution function of the longitudinal depletion force, $D_\parallel(F_\parallel)$. (b) Distribution function of the transverse depletion force, $D_\perp(F_\perp)$ (−), fit with a stretched exponential function with exponent $\beta = 1.5$ (green − − −), and fit with a Gaussian function (red · · ·). These curves refer to a value of density $\rho^* = 0.20$ and distance $R_{11} = 1$.

the fact that the distributions are becoming Gaussian only at very large values of density of depletants means that the fulfillment of the central limit theorem is slow for depletion interactions. For values of density of depletants $\rho^* \leq 0.3$, for which a liquid-like phase of large and small colloidal particles is expected to be stable,[11] the distribution functions are non-Gaussian. It is

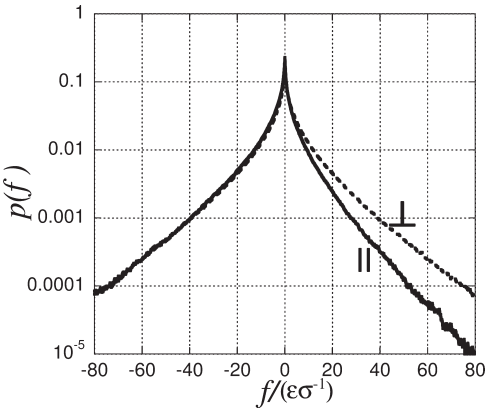

Figure 5. Distribution function of the longitudinal (−) and transverse (- - -) components of the force between a large sphere and a small sphere. Results obtained with the following parameters: $\kappa = (2)/(15)$, $n = 6$, $\rho^* = 0.26$, and $R_{11} = 0.8$.

therefore of interest to investigate the origin of the observed deviations from the Gaussian behavior at such values of density. In particular, one of the objectives of the next section is to establish whether these deviations solely derive from the fact the large particles interact only with a reduced number of small particles or if there is also an effect of the correlations between the depletants.

3.2. Distributions of Depletion Interactions: Analysis. Because depletion forces are collective in character, it is useful to analyze their distributions in terms of the distribution functions of the force that a single small particle exerts on a large particle. There are two types of these distributions: $p_\parallel(f_\parallel)$, the longitudinal distribution function of the singlet interactions resolved along the axis joining the two large particles, and $p_\perp(f_\perp)$, the transverse distribution function of the singlet interactions resolved along a direction perpendicular to the above-mentioned axis. Figure 5 provides examples of these singlet distribution functions. They have been calculated for a system of particles interacting via eq 1 with $\kappa = 2/15$ and $n = 6$, at a density of depletants $\rho^* = 0.26$ and $R_{11} = 0.8$. One can notice that $p_\parallel(f_\parallel)$ is asymmetric and that both singlet distributions show a considerable peak at $f_\parallel = f_\perp = 0$.

If the small particles were noninteracting between them, then the distributions of the collective depletion forces would be given by the convolution of the pdf's of the single-particle force.[29] This means that the Fourier transforms of the collective force pdf are just the product of the Fourier transforms of the pdf's of the single-particle force, $\tilde{p}_\parallel(\omega)$ and $\tilde{p}_\perp(\omega)$.

Because the singlet longitudinal distribution is generally asymmetric, its Fourier transform has a real, $\mathcal{R}\,\tilde{p}_\parallel(\omega)$, and an imaginary, $\mathcal{I}\,\tilde{p}_\parallel(\omega)$, part. It is therefore convenient to define a modulus:

$$|\tilde{p}_\parallel(\omega)| = [(\mathcal{R}\tilde{p}_\parallel(\omega))^2 + (\mathcal{I}\tilde{p}_\parallel(\omega))^2]^{1/2} \quad (2)$$

and a phase:

$$\phi_\parallel(\omega) = \tan^{-1}\left(\frac{\mathcal{I}\tilde{p}_\parallel(\omega)}{\mathcal{R}\tilde{p}_\parallel(\omega)}\right) \quad (3)$$

From these quantities, one can obtain, respectively, the modulus, $|\tilde{\Pi}_\parallel(\omega)|$, and the phase, $\Phi_\parallel(\omega)$, of the Fourier transform of the distribution of the collective force by performing the following

dx.doi.org/10.1021/jp2005259 |J. Phys. Chem. B 2011, 115, 6608–6615

sums:

$$|\tilde{\Pi}_{\|}(\omega)| = \sum_N |\tilde{p}_{\|}(\omega)|^N \nu(N) \quad (4)$$

$$\Phi_{\|}(\omega) = \sum_N \phi_{\|}(\omega) N \nu(N) \quad (5)$$

with $\nu(N)$ the pdf of having N small spheres inside the interaction range of a large sphere. One example of a normalized to unity $\nu(N)$ is provided in Figure 6.

The Fourier transform of the longitudinal distribution of the collective force has a real part, given by:

$$\mathcal{R}\tilde{\Pi}_{\|}(\omega) = |\tilde{\Pi}_{\|}(\omega)|\cos \Phi_{\|}(\omega) \quad (6)$$

and an imaginary part, given by:

$$\mathcal{I}\tilde{\Pi}_{\|}(\omega) = |\tilde{\Pi}_{\|}(\omega)|\sin \Phi_{\|}(\omega) \quad (7)$$

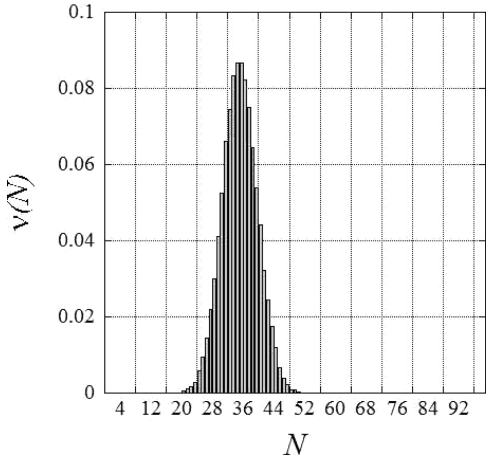

Figure 6. Normalized form of the distribution $\nu(N)$ for the case $\kappa = 2/15$, $n = 6$, $\rho^* = 0.26$, and $R_{11} = 0.8$.

The sum of the inverse Fourier transforms of $\mathcal{R}\tilde{\Pi}_{\|}(\omega)$ and $\mathcal{I}\tilde{\Pi}_{\|}(\omega)$ finally provides the distribution of the longitudinal depletion force, $\Pi_{\|}(F_{\|})$, reconstructed from $p_{\|}(f_{\|})$.

Because the singlet transverse distribution is symmetric, its Fourier transform has only the real part, and the Fourier transform of the transverse distribution of the collective force is given by:

$$\tilde{\Pi}_{\perp}(\omega) = \sum_N \tilde{p}_{\perp}(\omega)^N \nu(N) \quad (8)$$

The inverse Fourier transform of $\tilde{\Pi}_{\perp}(\omega)$ provides $\Pi_{\perp}(F_{\perp})$, the distribution of the transverse depletion force reconstructed from the $p_{\perp}(f_{\perp})$.

It has also been verified that a very good approximation to $\tilde{\Pi}_{\|,\perp}(\omega)$ is provided by:

$$|\tilde{\Pi}_{\|,\perp}(\omega)| \simeq |\tilde{p}_{\|,\perp}(\omega)|^{\langle N \rangle} \quad (9)$$

where $\langle N \rangle$ is the mean value of N. The goodness of this approximation together with eq 5 are encouraging in view of a possible implementation of this approach using experimental data, as discussed below.

The reconstructed pdf's $\Pi_{\|}(F_{\|})$ and $\Pi_{\perp}(F_{\perp})$ are to be compared to the corresponding distributions calculated during the course of the MD simulations. This comparison has been done for a large set of cases, distinguished by the values of n, ρ^*, R_{11} but all referring to a value of $\kappa = 2/15$.

Figure 7 provides $D_{\|}(F_{\|})$, $\Pi_{\|}(F_{\|})$, and the difference $D_{\|}(F_{\|}) - \Pi_{\|}(F_{\|})$ for $R_{11} = 0.6$ and different values of the parameter regulating the softness of the direct interactions and the density of depletants. There are very small yet noticeable differences between the distributions of the longitudinal depletion force calculated in the MD simulations and the respective reconstructions from $p_{\|}(f_{\|})$. While these differences are slightly decreasing with the density, they do not appear to depend on n.

The same insensitivity of the results on the softness of the direct interactions also holds for the transverse distributions.

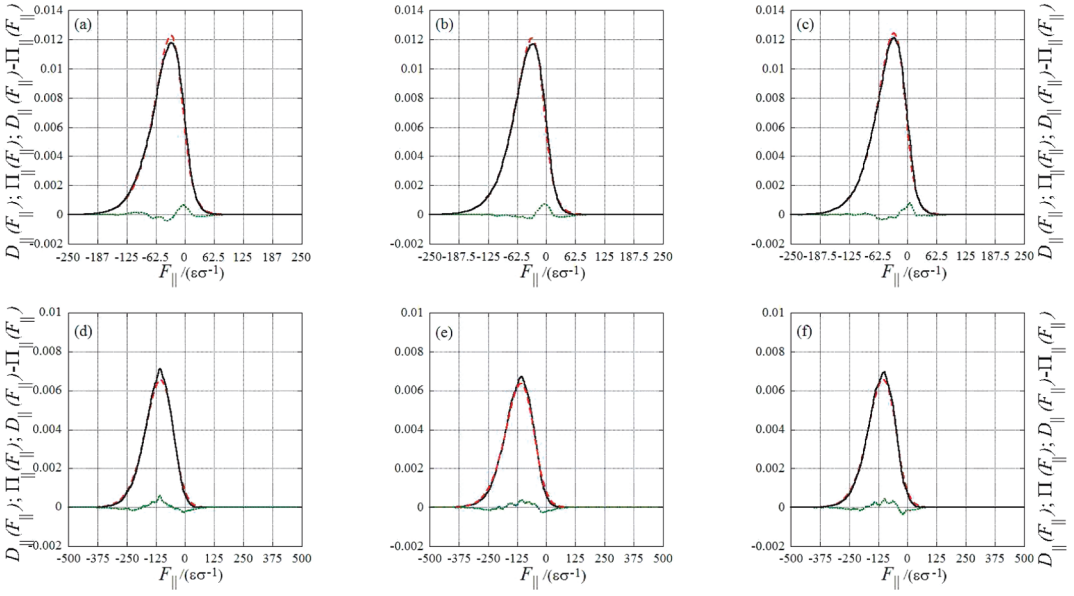

Figure 7. Distribution of the longitudinal depletion force, as calculated in the MD simulations, $D_{\|}(F_{\|})$ (—), reconstructed, $\Pi_{\|}(F_{\|})$ (red – – –), and their difference (green · · ·), for $R_{11} = 0.6$ and the following values of n and density: (a) $n = 3$, $\rho^* = 0.13$; (b) $n = 6$, $\rho^* = 0.13$; (c) $n = 12$, $\rho^* = 0.13$; (d) $n = 3$, $\rho^* = 0.26$; (e) $n = 6$, $\rho^* = 0.26$; (f) $n = 12$, $\rho^* = 0.26$.

dx.doi.org/10.1021/jp2005259 |J. Phys. Chem. B 2011, 115, 6608–6615

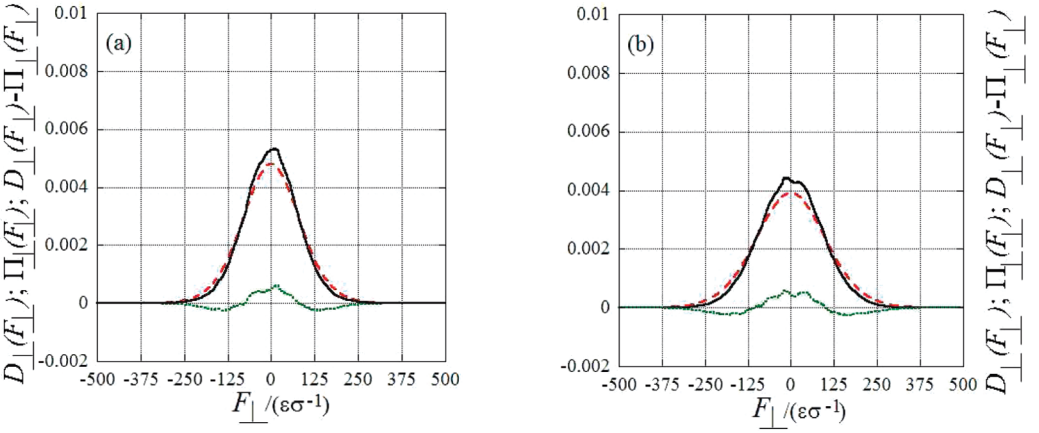

Figure 8. Distribution of the transverse depletion force: calculated in the MD simulations, $D_\perp(F_\perp)$ (−), reconstructed, $\Pi_\perp(F_\perp)$ (red − − −), and their difference (green ···), for R_{11} = 0.8 (a) and 1.3 (b). In both cases, n = 6 and ρ^* = 0.3.

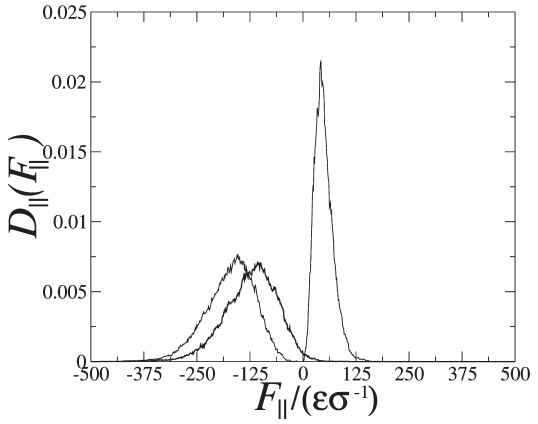

Figure 9. The distribution of the longitudinal depletion force as in panel (e) of Figure 7 (bold), the pdf's obtained with only the contributions from particles between the large spheres (thin curve on the right) and outside the large spheres (thin curve on the left); see text.

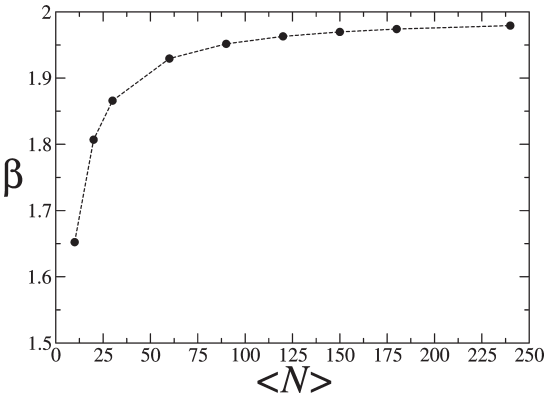

Figure 10. Exponent of the stretched exponential as a function of ⟨N⟩ used in eq 9 to reconstruct the collective longitudinal depletion force distribution from the single particle data of Figure 5.

Figure 8 provides $D_\perp(F_\perp)$, $\Pi_\perp(F_\perp)$, and their difference $D_\perp(F_\perp) - \Pi_\perp(F_\perp)$ for n = 6, ρ^* = 0.3, and two values of R_{11}. It would appear that the difference $D_\perp(F_\perp) - \Pi_\perp(F_\perp)$ is insensitive to R_{11}, as expected on the basis of symmetry arguments. Perhaps surprisingly, the absolute value of the difference between calculated and reconstructed distributions is slightly larger in the transverse case than in the longitudinal case for the same values of parameters. This can be appreciated, for instance, by comparing panel (e) of Figure 7 with panel (a) of Figure 8.

The parallel component of the fluctuating force acting on one of the large spheres shown in panel (e) of Figure 7 has been decomposed into contributions due to internal and external small particles. Internal particles are those that lie in the region of space defined by two parallel planes that pass through the center of the large spheres and are orthogonal to the axis joining them. A positive sign of the force identifies internal small particles. These data have been computed in a shorter run, so the curve of the total force is less smooth than that of panel (e) in Figure 7. The deviation of these pdf's from a Gaussian has been measured through the parameter α_2,[30] with values of 0.48 for the internal particles, 0.22 for the external ones, and 0.20 for the total curve, which is the convolution of the first two. Apparently, the largest deviation from a Gaussian behavior pertains to the internal particles, which more directly feel an inhomogeneous environment.

If the small particles were uncorrelated, one would expect that the reconstructed distribution matched the corresponding calculated distribution. The fact that this does not happen is a signature of the correlations, that is, the interactions, between the depletants. These correlations therefore contribute, albeit to a little extent, to the slow fulfilment of the central limit theorem, largely to be ascribed to the reduced number of depletants that, at each instant, interact with the large object.

The rate at which the Gaussian limit is approached can be appreciated from Figure 10. This plot shows the value of β, the exponent of the stretched exponential used to fit the collective pdf $|\tilde{\Pi}_\parallel(\omega)|$ computed according to eq 9, for various values of the average number of neighbors.

It appears that some 100 neighbors would be required to reach a substantially Gaussian behavior, while we have ⟨N⟩ ≃ 34 (Figure 6) with a size ratio of 7.5. This means that a truly Gaussian behavior can only be obtained with much larger values of this ratio if the density is kept in the same range.

Another route to appreciating the approach to the limiting Gaussian behavior is provided by time averaging the depletion force before its probability distribution is computed. Figure 11

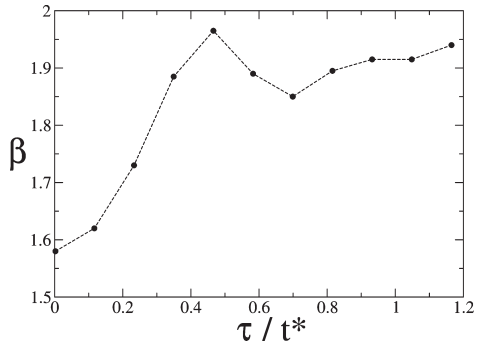

Figure 11. Exponent of the stretched exponential as a function of the time window, τ, used to average the transverse component of the depletion force. The circles indicate actual values of the time window, while the dashed line is just a guide to the eye.

shows β, the exponent of the stretched exponential used to fit the pdf of the transverse component of the depletion force, as a function of the time window, τ, used for averaging. β depends on τ in a nonmonotonic way: it increases rapidly up to a maximum very close to 2 at $\tau = 0.47t^*$, and then, after a minimum at $\tau = 0.7t^*$, it returns to values that allow the corresponding pdf to be safely considered Gaussian. The relaxation time of the autocorrelation function of the transverse force turns out to be $0.55t^*$, and it vanishes in the noise before $2.3t^*$, according to preliminary results.[31] Hence, for the transverse component, the picture of a depletion force that only after losing memory of its initial value gives a Gaussian static pdf appears consistent with the available data.

The autocorrelation function of the longitudinal component, on the other hand, shows a weak, but significant, negative long-time tail, that extends up to $7t^*$ for both big spheres. In fact, coarse grained pdf's, where the longitudinal force is averaged over such a time scale, keep their asymmetry so they cannot, strictly speaking, be considered Gaussian. This behavior is currently under further analysis.[31]

Having seen that the reconstruction method works substantially well for the distributions of both longitudinal and transverse component of the depletion force, it is now of interest to note that, in the case of purely repulsive direct interactions between the particles, there exists a one-to-one correspondence between the magnitude of the force that a single small particle exerts on a large particle, $p(|f(r)|)$, and their distance, r. This means that the pair distribution function between large and small spheres, $g(r)$, and the pdf of the magnitude of the force can be related through the "change-of-variable formula",[32] which in this case reads:

$$p(|f(r)|)\, \mathrm{d}|f(r)| \propto \rho g(r) r^2\, \mathrm{d}r \qquad (10)$$

where ρ is the density of small spheres. The proportionality factor is set by the normalization condition.

Figure 12 shows an application of this equation, to both obtain $g(r)$ from the pdf of the magnitude of the force, computed in the MD run, and to reconstruct the latter from the MD $g(r)$. The agreement is quantitative, except for the noise in the MD $g(r)$, simply due to statistics, admittedly poor yet sufficient for the present demonstration purpose.

Pair correlation functions can be experimentally determined. Traditionally, they have been obtained by Fourier transforming the stucture factors, $S(k)$, derived from scattering techniques.[33] Recently, real-space confocal microscopy techniques have been

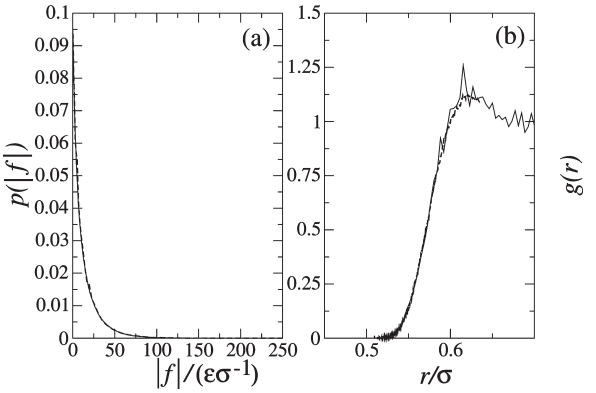

Figure 12. Directly calculated (—) and reconstructed (- - -) pdf of the magnitude of the force (a) and $g(r)$ between a large sphere and a small sphere (b). The reconstructed $g(r)$ ends where the force vanishes (eq 10).

employed,[34] to also obtain the $g(r)$ for the large colloid−small colloid pairs in a colloidal mixture, whose interactions closely resemble our model short-range repulsions.

From the $g(r)$ of a real colloidal system, $p(|f(r)|)$ can be derived, provided that $u_{12}(r)$ is known. This can be determined by inverting the measured $g(r)$ via suitable integral equation techniques,[33] or, as in ref 35, by extrapolating to vanishingly small volume fraction the measured potential of mean force. From $p(|f(r)|)$ and applying the reconstruction procedure, one could arrive at a good approximation of the distribution of the magnitude of the depletion force, $D(|F|)$, that real depletants induce on two big colloids.

Provided the two large particles can be constrained to stay in a geometrical arrangement similar to that adopted in this work (e.g., by means of optical tweezers[36]), it could become feasible measuring the orientationally dependent pair correlation function $g(\mathbf{r})$, as also anticipated in ref 34. This would provide information on not only radial but also angular correlations between big and small spheres. From this, the distribution functions $p_{\parallel}(f_{\parallel})$ and $p_{\perp}(f_{\perp})$ could be obtained. Next, by applying the reconstruction method, one would arrive at estimates of $D_{\parallel}(F_{\parallel})$ and $D_{\perp}(F_{\perp})$.

Confocal microscopy technique would seem better suited to achieve the above-mentioned tasks. It has the advantage, over scattering techniques, of being able to track particle coordinates, as is done in numerical simulations. Within the confocal microscopy technique, therefore, distribution functions of depletion interactions would be directly obtainable, allowing for a comparison between them and those reconstructed from the $g(r)$'s.

4. CONCLUSIONS

Model colloidal binary mixtures have been simulated via the molecular dynamics method. The mixtures comprise two large spherical particles immersed in a bath of small spherical particles, the interactions between these particles being soft repulsive.

The object of the work has been the calculations of the distribution functions of the effective depletion forces that the small spheres induced on the large spheres.

In general, the distribution functions are non-Gaussian. This is predominantly due to the intrinsically too small number of small spheres surrounding the large spheres when realistic densities of

the small spheres are considered to have the binary mixtures in the stable fluid region of the phase diagram.

We have found that if the pdf is calculated after taking a time average of the fluctuating force, the Gaussian form can be recovered on a time scale of unity (in reduced units) for the transverse component. On the contrary, the longitudinal component, the actual depletion force, keeps being nonsymmetrical on a longer time scale. It appears then that, even in a system with short-range repulsive forces, either an average over a fairly long time scale or one over a significantly larger number of neighbors (i.e., a larger density of small spheres or a much bigger large sphere) is necessary for the pdf of the depletion force to become truly Gaussian.

The behavior of the static distribution functions suggests that similar deviations from a Gaussian form can be found in the dynamics of depletion forces. Actually, preliminary results confirm that the four-time correlation functions of the depletion forces show non-Gaussian features. We plan to include these results in a future paper,[31] where we will also attempt to study the transition from single-particle to collective dynamics through the intermediate scattering function, $F(k,t)$, and its self-part $F_s(k,t)$.

The distribution functions of depletion forces have been analyzed in terms of the distribution function of the force that a single small sphere exerts on a large sphere. The reconstruction method able to obtain the distribution function of the collective force from the distribution of the single force has been successfully tested.

The relationships between the distribution function of the single force and the radial-angular pair correlation function between a large and a small sphere, combined with the reconstruction method, make the distribution functions of the depletion forces in real colloidal mixtures experimentally accessible with usual reciprocal-space techniques. Modern real-space techniques, able to track particle coordinates as in a numerical simulation, would not need such a reconstruction procedure as they should be able to sample directly the various distribution functions. It is hoped that the present results on model colloids will stimulate such experiments on real colloids.

AUTHOR INFORMATION

Corresponding Author

*E-mail: tani@dcci.unipi.it.

Present Addresses

[†]Dipartimento di Chimica, Università di Pisa, Via Risorgimento 35, I-56126 Pisa, Italy. E-mail: giorgio.cinacchi@bristol.ac.uk.

ACKNOWLEDGMENT

Italian MIUR is gratefully acknowledged for financial support through PRIN 2007 "Energy, charge and mass transfer in complex systems". G.C. acknowledges the financial support of the European Commission via a Marie Curie Intra-European Research Fellowship, project number PIEF-GA-2007-220557, during which part of this work was carried out. Prof. R. Evans and Dr. C. P. Royall (University of Bristol) are thanked for useful discussions.

REFERENCES

(1) Asakura, S.; Oosawa, F. *J. Chem. Phys.* **1954**, *22*, 1255. Asakura, S.; Oosawa, F. *J. Polym. Sci.* **1958**, *33*, 183.
(2) Vrij, A. *Pure Appl. Chem.* **1976**, *48*, 471.
(3) Likos, C. N. *Phys. Rep.* **2001**, *348*, 267.
(4) Denton, A. R. In *Nanostructured Soft Matter: Experiment, Theory, Simulation and Perspectives*; Zvelindovsky, A. V., Ed.; Springer: Dordrecht, 2007; pp 395−433.
(5) Biben, T.; Hansen, J. P. *J. Phys.: Condens. Matter* **1991**, *3*, F65.
(6) Dijkstra, M.; van Roij, R.; Evans, R. *Phys. Rev. E* **1999**, *59*, 5744.
(7) Attard, P. *J. Chem. Phys.* **1989**, *91*, 3083. Attard, P.; Patey, G. N. *J. Chem. Phys.* **1990**, *92*, 4970.
(8) Roth, R.; Evans, R.; Dietrich, S. *Phys. Rev. E* **2000**, *62*, 5360.
(9) Biben, T.; Bladon, P.; Frenkel, D. *J. Phys.: Condens. Matter* **1996**, *8*, 10799.
(10) Dickman, R.; Attard, P.; Simonian, V. *J. Chem. Phys.* **1997**, *107*, 205.
(11) Cinacchi, G.; Martinez-Raton, Y.; Mederos, L.; Navascues, G.; Tani, A.; Velasco, E. *J. Chem. Phys.* **2007**, *127*, 214501.
(12) Kaplan, P. D.; Faucheux, L. P.; Libchaber, A. J. *Phys. Rev. Lett.* **1994**, *73*, 2793.
(13) Ohshima, Y. N.; Sakagami, H.; Okumto, K.; Tokoyoda, A.; Igarashi, T.; Shintaku, K. B.; Toride, S.; Sekino, H.; Kabuto, K.; Nishio, I. *Phys. Rev. Lett.* **1997**, *78*, 3963.
(14) Rudhardt, D.; Bechinger, C.; Leiderer, P. *Phys. Rev. Lett.* **1998**, *81*, 1330.
(15) Crocker, J. C.; Matteo, J. A.; Dinsmore, A. D.; Yodh, A. G. *Phys. Rev. Lett.* **1999**, *82*, 4352.
(16) Kleshchanok, D.; Tuinier, R.; Lang, P. R. *J. Phys.: Condens. Matter* **2008**, *20*, 073101.
(17) Bartolo, D.; Ajdari, A.; Fournier, J. P.; Golestanian, R. *Phys. Rev. Lett.* **2002**, *89*, 230601.
(18) Vliegenthart, G. A.; van der Schoot, P. *Europhys. Lett.* **2003**, *62*, 600.
(19) Izvekov, S.; Voth, G. A. *J. Chem. Phys.* **2006**, *125*, 151101.
(20) Hijón, C.; Español, P.; Vanden-Eijnden, E.; Delgado-Buscalioni, R. *Faraday Discuss.* **2010**, *144*, 301.
(21) Marconi, U. M. B.; Puglisi, A.; Rondoni, L.; Vulpiani, A. *Phys. Rep.* **2008**, *461*, 111.
(22) Hill, T. L. *J. Chem. Phys.* **1962**, *36*, 3182.Hill, T. L. *Thermodynamics of Small Systems*; Dover: New York, 1994.
(23) Hill, T. L.; Chamberlin, R. V. *Proc. Natl. Acad. Sci. U.S.A.* **1998**, *95*, 12779. Hill, T. L. *Nano Lett.* **2001**, *1*, 273. Schnell, S. K.; Vlugt, T. J. H.; Simon, J. M.; Bedeaux, D.; Kjelstrup, S. *Chem. Phys. Lett.* **2011**, *504*, 199.
(24) Haile, J. M. *Molecular Dynamics Simulation: Elementary Methods*; Wiley: New York, 1997. Rapaport, D. C. *The Art of Molecular Dynamics Simulation*; Cambridge University Press: Cambridge, 2004.
(25) Berendsen, H. J. C.; Postma, J. P. M.; van Gunsteren, W. F.; Di Nola, W. F.; Haak, J. R. *J. Chem. Phys.* **1984**, *81*, 3684.
(26) Ryckaert, J. P.; Ciccotti, G.; Berendsen, H. J. C. *J. Comput. Phys.* **1977**, *23*, 327.
(27) http://ganter.chemie.uni-dortmund.de/MOSCITO/.
(28) Ciccotti, G.; Ferrario, M.; Hynes, J. T.; Kapral, R. *Chem. Phys.* **1989**, *129*, 241.A comprehensive review of these methods is given by: Darve, E. In *Free Energy Calculations*; Chipot, C., Pohorille, A., Eds.; Springer: Berlin, 2007; pp 119−170.
(29) Severini, T. A. *Elements of Distribution Theory*; Cambridge University Press: Cambridge, 2005.
(30) Rahman, A. *Phys. Rev. A* **1964**, *136*, 405.
(31) Bertolini, D.; Cinacchi, G.; Tani, A., unpublished work.
(32) This topic is discussed in many textbooks, see, for example: Stirzaker, D. *Elementary Probability*, 2nd ed.; Cambridge University Press: Cambridge, 2003; Chapter 7. Risken, H. *The Fokker-Planck Equation*, 2nd ed.; Springer: Berlin, 1989; Chapter 2.
(33) Hansen, J. P.; Mc Donald, I. R. *Theory of Simple Liquids*; Academic Press: London, 1986.
(34) Royall, C. P.; Louis, A. A.; Tanaka, H. *J. Chem. Phys.* **2007**, *127*, 044507.
(35) Iacovella, C. R.; Rogers, R. E.; Glotzer, S. C.; Solomon, M. J. *J. Chem. Phys.* **2010**, *133*, 164903.
(36) Grier, D. G. *Nature* **2003**, *424*, 810.